

# Measurement of Wave Coherence Using Spaceborne Synthetic Aperture Radar

Frank Monaldo and Donald Thompson  
The Johns Hopkins University Applied Physics Laboratory  
11100 Johns Hopkins Road Laurel MD 20723-6099  
phone: (240) 228-8648 fax: (240) 228-5548  
email: [f.monaldo@jhuapl.edu](mailto:f.monaldo@jhuapl.edu) and [d.thompson@jhuapl.edu](mailto:d.thompson@jhuapl.edu)  
Award Number: N00014-98-D-8124  
<http://fermi.jhuapl.edu>

## LONG-TERM GOALS

The United States Navy is evaluating the feasibility of constructing and deploying very large mobile offshore bases (MOBs). Such platforms may be 1.5 km long and 300 m wide. These structures fall far outside the scope of typical maritime design experience. Proper design depends upon the ability to characterize ocean wave fields, particular nonlinear features like wave “long crestedness” and wave “groupiness.” A long-term goal is to provide such characterizations.

## OBJECTIVES

The specific objective of this work is to develop and apply techniques for the objective estimation of wave long crestedness and wave groupiness from spaceborne synthetic aperture radar (SAR) data of ocean surface waves. Spaceborne SAR imagery offers the unique combination of high resolution (25 m) and large swath (100 km) necessary to measure large scale wave coherence.

## APPROACH

The authors listed above are the primary contributors to this work. The basic approach here is two fold. First, develop techniques to objectively measure two properties of wave coherence: ocean wave crest length and long crestedness. Second, apply these techniques to spaceborne SAR imagery. The difference between crest lengths and wave groupiness observed in SAR imagery and those predicted by linear theory is a measure of wave coherence caused by nonlinear wave-wave interaction.

## WORK COMPLETED

### SAR Wave Measurement

Ocean waves are typically measured at a single location as a function of time. However, assessment of the spatial coherence of waves requires measurement of the two-dimensional surface wave field. Spaceborne SARs offer important advantages in measuring spatial coherence: (1) They have sufficient resolution (typically 25 m) to capture ocean wave patterns. (2) Spaceborne SAR image swaths are typically 100 km wide or larger, providing a synoptic view of the wave field. (3) The global coverage of spaceborne SARs allows the acquisition of ocean imagery in the midst of storms.

# Report Documentation Page

Form Approved  
OMB No. 0704-0188

Public reporting burden for the collection of information is estimated to average 1 hour per response, including the time for reviewing instructions, searching existing data sources, gathering and maintaining the data needed, and completing and reviewing the collection of information. Send comments regarding this burden estimate or any other aspect of this collection of information, including suggestions for reducing this burden, to Washington Headquarters Services, Directorate for Information Operations and Reports, 1215 Jefferson Davis Highway, Suite 1204, Arlington VA 22202-4302. Respondents should be aware that notwithstanding any other provision of law, no person shall be subject to a penalty for failing to comply with a collection of information if it does not display a currently valid OMB control number.

1. REPORT DATE <b>30 SEP 1999</b>		2. REPORT TYPE		3. DATES COVERED <b>00-00-1999 to 00-00-1999</b>	
4. TITLE AND SUBTITLE <b>Measurement of Wave Coherence Using Spaceborne Synthetic Aperture Radar</b>				5a. CONTRACT NUMBER	
				5b. GRANT NUMBER	
				5c. PROGRAM ELEMENT NUMBER	
6. AUTHOR(S)				5d. PROJECT NUMBER	
				5e. TASK NUMBER	
				5f. WORK UNIT NUMBER	
7. PERFORMING ORGANIZATION NAME(S) AND ADDRESS(ES) <b>Johns Hopkins University, Applied Physics Laboratory, 11100 Johns Hopkins Road, Laurel, MD, 20723</b>				8. PERFORMING ORGANIZATION REPORT NUMBER	
9. SPONSORING/MONITORING AGENCY NAME(S) AND ADDRESS(ES)				10. SPONSOR/MONITOR'S ACRONYM(S)	
				11. SPONSOR/MONITOR'S REPORT NUMBER(S)	
12. DISTRIBUTION/AVAILABILITY STATEMENT <b>Approved for public release; distribution unlimited</b>					
13. SUPPLEMENTARY NOTES					
14. ABSTRACT					
15. SUBJECT TERMS					
16. SECURITY CLASSIFICATION OF:			17. LIMITATION OF ABSTRACT	18. NUMBER OF PAGES	19a. NAME OF RESPONSIBLE PERSON
a. REPORT <b>unclassified</b>	b. ABSTRACT <b>unclassified</b>	c. THIS PAGE <b>unclassified</b>			

The study of mechanisms for SAR wave begins in 1977 with the description by Elachi and Brown [1]. Their approach, with a considerable refinement, remains valid today. Additional work by many others has filled in the gaps [2–5]. According to Bragg scattering theory, the radar cross section in a SAR image is proportional to the roughness on the ocean surface at the radar wavelength projected on the surface. For near-nadir incidence ( $20^\circ$  to  $25^\circ$ ), the wave imaging is dominated by “tilt modulation” for range (cross-track) traveling waves. Specifically, the wave-induced modulation of radar cross section (image intensity) is proportional to the tilt or slope changes of the long ocean surface waves. There is high confidence in the ability of a SAR to faithfully image range-traveling waves.

Azimuth wave imaging is intrinsically tied to how a SAR image is formed [6, 7]. A SAR relies on Doppler information to achieve fine-scale azimuth resolution. As an azimuth-traveling wave propagates it advects the surface so that a component of the periodic wave orbital velocity is moving along the SAR line-of-sight. This causes the apparent azimuth positions of scatterers to be displaced in the SAR image. The periodic ocean wave motion moves scatterers in such a way as to concentrate and dilute the apparent density of the scatterers in the SAR image at the spatial frequency of the long waves. This renders azimuth-traveling waves visible in SAR imagery. This imaging mechanism is known as “velocity-bunching.” The velocity-bunching effect is proportional to both the orbital velocities of the long waves and to  $R/V$ , where  $R$  is range from the SAR platform to the surface and  $V$  is the radar ground velocity. When waves and  $R/V$  grow large, the azimuth shifts can become large enough to smear the image and significantly degrade the azimuth resolution.

A useful guide to the magnitude of this degradation is the equation  $\lambda_{\min} = (R/V)H_s^{1/2}$  where  $\lambda_{\min}$  is the minimum detectable azimuth wavelength and  $H_s$  is the significant wave height (SWH). Clearly, the higher the sea state and the larger the  $R/V$  ratio are, the larger the minimum detectable azimuth wavelength is. For a high altitude (800 km) SAR platform like ERS-1/2 or Radarsat,  $R/V$  equals 120 s. The minimum detectable azimuth wavelength varies from 170 m to 380 m for SWHs from 2 m to an extreme of 10 m. Thus, even under extreme conditions, high-altitude SARs should be able to image azimuth-traveling waves at wavelengths that will resonate with MOBs. SAR wave imaging at lower altitudes, such as the 200-km shuttle altitude, offers greater fidelity in wave measurement.

### **Crest Length Measurement**

One aspect of wave coherence is wave “long crestedness.” To economically assess wave long crestedness requires the development of automated procedures that produce long-crestedness parameters from image archives with minimal human intervention.

The challenge of arriving at a statistical description of long wave crests is non-trivial. We present here a rigorous and repeatable procedure for identification and measurement wave crests in imagery. This procedure is dependent on the discretionary selection of only a few key parameters. Although a unambiguous formal definition of long crestedness may exceed our grasp, it is possible to compare observed long-crestedness with the long-crestedness expected if ocean surface waves were purely linear. Here, we describe this procedure and apply it to a sample SAR image from Hurricane Josephine acquired during the Shuttle Imaging Radar-B (SIR-B) mission.

The extraction of crest length statistics from SAR imagery involves two basic steps: (1) the filtering of a SAR image so that crests are conspicuously identified as separate “blobs,” and (2) the measurement of crest length from these blobs.

**Wavenumber Domain Filtering.** We first Fourier transform SAR image intensity so that filters are applied in the wavenumber domain. Let  $I(x, y)$  represent SAR image intensity as a function of range,  $x$ , and azimuth,  $y$ , position. We represent the Fourier transform of  $I(x, y)$  by  $F(k_x, k_y)$  where  $k_x$  and  $k_y$  are range and azimuth wavenumber, respectively. If we let  $k_{\min}$  represent the minimum wavenumber at which we want information, we can construct a high-pass filter  $H_1(k_x, k_y)$  such that  $H_1(k_x, k_y) = 1$  for  $k \geq k_{\min}$  and 0 elsewhere, where  $k$  is wavenumber magnitude. Typically, we set  $k_{\min} = 2\pi / 1600$  r/m. To remove the remaining noise we threshold based on the values in the image spectrum,  $F^2(k_x, k_y)$ . We define a threshold level by  $T_s = \mu_s + A\sigma_s$  where  $\mu_s$  is the mean spectral value,  $\sigma_s$  is the standard deviation of the spectrum, and  $A$  is an adjustable parameter, typically set to 3. This second spectral filter is defined as  $H_2(k_x, k_y) = 1$  for  $F^2(k_x, k_y) \geq T_s$  and 0 elsewhere. By application of these filters, we generate a new Fourier transform,  $F'(k_x, k_y)$ .

**Image Domain Filtering.** We produce a filtered SAR image by computing the inverse Fourier transform of  $F'(k_x, k_y)$ . To separate crest from non-crest areas, we applied a threshold to the resulting image. If  $\mu_1$  is the mean of the filtered image and  $\sigma_1$  its standard deviation, then the threshold level is  $T_1 = \mu_1 + B\sigma_1$  where  $B$  is an adjustable, typical set to 1. Portions of the image greater than threshold are set to 1, otherwise they are set to 0. Each contiguous area of 1's is a “blob.”

**Blob Identification and Measurement.** There are standard image processing procedures that are able to find contiguous regions or blobs in an image and label them sequentially. We then fit each blob to an ellipse. For each such ellipse we determine the semi-major and semi-minor axes, the eccentricity, and the orientation of the ellipse. Twice the semi-major axis is the crest length. Here we apply the procedure to a  $25.6 \times 25.6$  km area to the Hurricane Josephine SAR imagery. After full processing of this image, we obtain a list of all the wave crests in the image and their dimensions.

Wave-wave interactions conspire to bunch waves up and create wave crest lengths, which differ from what might be expected if all wave frequency components acted independently. By using a simulation technique, we are able to compare the observed crest length statistics, with similar statistics that would be generated from images having the same spectrum but whose frequency components are independent.

We begin this simulation by using the spectrum computed from observed image. We assume that this spectrum is but one realization of the ensemble mean spectrum, which represents the surface. In this single realization, each spectral element is random variable having a  $\chi^2$ -distribution with 2 degrees of freedom. The mean of this distribution is the ensemble mean spectral value. We approximate this ensemble mean spectrum by smoothing the observed spectrum. The aim is to produce new simulated images with the following properties: (1) The ensemble of mean spectrum of similar images equals the observed image spectrum. (2) Each spectral component is independent of the others, *i.e.* the phase of each spectral element is independent of all other phases.

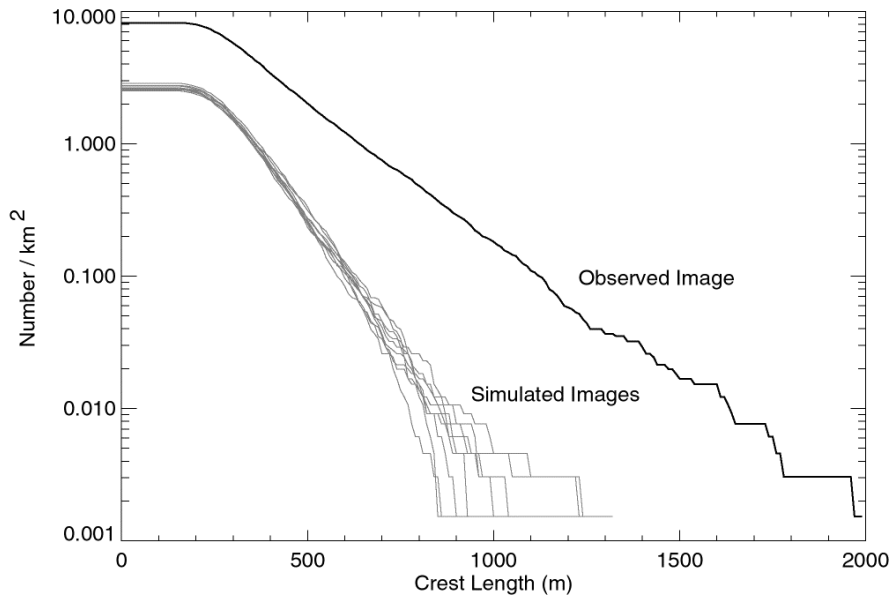


**Fig. 1:** *The number of wave crests encountered longer than the abscissa per square kilometer.*

Results indicate that very long wave crests are more common on the ocean than would be expected if wave components were independent. Fig. 1 shows the number of wave crests longer than the abscissa that will be found on average in one square kilometer. The higher curve was computed from the original SAR image, while the lower curves were the result of simulations. The two curves represent the observed and simulated images. From Fig. 1, we may infer that in the observed image one is likely to encounter two wave crests longer 1000 m in a  $10 \text{ km}^2$  area. In the simulated images, it is not likely that a single such wave crest would be encountered.

### Wave Groupiness Measurement

Wave groupiness is the likelihood that large waves will group together in a series [8]. Any offshore platform will have more difficulty if especially large waves are grouped together possibly setting up a resonance. We suspected that wave groupiness might be apparent in the two-dimensional autocorrelation function. Fig. 2A represents the two-dimensional autocorrelation function of an image near Hurricane Josephine. At the center, or zero spatial lag, there are local correlations on scales of a few hundred meters. This corresponds to the existence of ocean waves in the image. Put more simply, a wave crest at any particular position is correlated with other wave crests one, two, or more wavelengths away. The correlation decreases as one moves farther away.

Upon more careful examination of this two-dimensional autocorrelation, groups or packets of waves are visible. This is a consequence of wave groupiness. By rotating the autocorrelation function shown in Fig. 2A so that the crests are horizontal and collapsing this two-dimensional representation to one dimension, the groups become more apparent. Fig. 2B is a plot of the one-dimensional autocorrelation function. Again we note the oscillations near zero lag associated with surface waves. The envelope of the oscillations is the signature of groupiness. It has a spatial period of 2.5 km. Hence, for this particular wave field, one would expect especially large groups of waves separated by 2.5 km, about 10 wave periods.

Autocorrelations computed from simulated wave images based on linear theory did not exhibit this groupiness behavior. This is additional evidence that empirical data, rather than linear wave theory is needed to estimate wave groupiness.

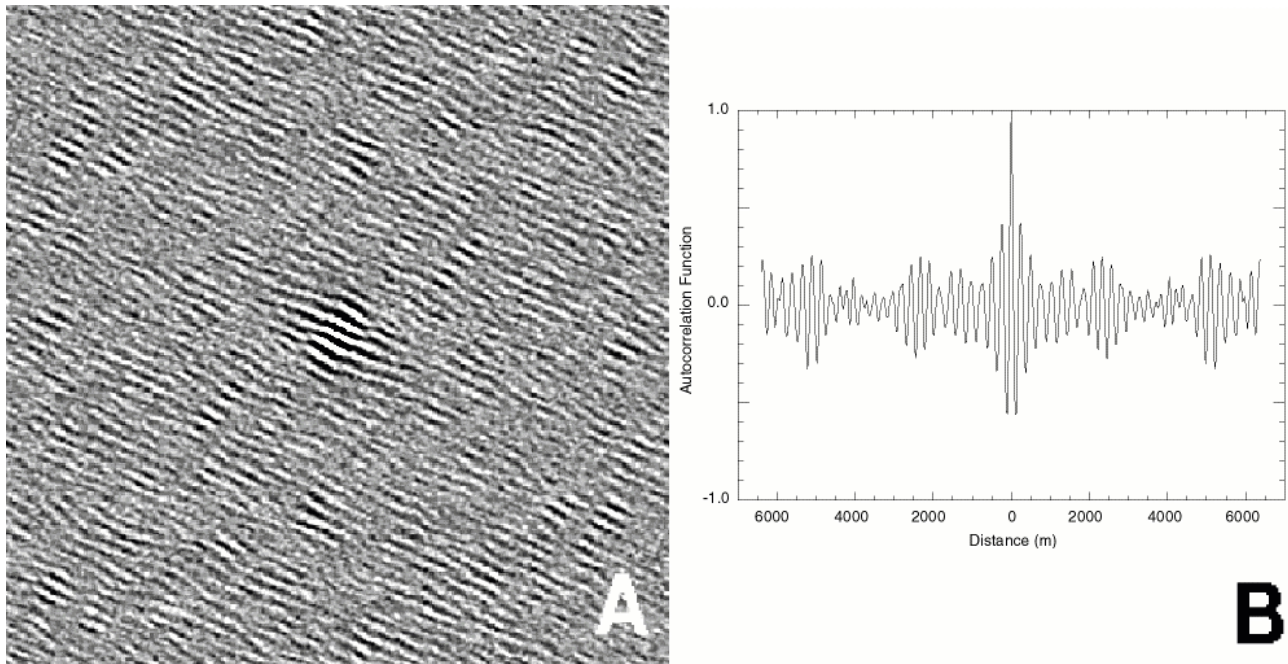


*Fig 2. A two-dimensional autocorrelation function (A) and one-dimensional autocorrelation function (B).*

## RESULTS

Spaceborne SAR images offer the prospect of measuring ocean surface waves on scales and at resolutions necessary to make judgments about the effect of waves on very large offshore platforms. This past year has been occupied developing the repertoire of image processing tools necessary to measure waves coherence properties from SAR images. Preliminary evaluation of imagery in the vicinity of Hurricane Josephine indicates that waves exhibit both longer crest lengths and more groupiness than would be expect on the basis of linear theory alone. It is clear that wave imagery will be necessary to characterize properties of wave coherence. At JHU/APL, we have acquired SAR ocean wave data sets from Hurricanes Josephine, Bonnie, Danielle, and Edouard. In the coming year, we plan to compute the crest length statistics and autocorrelation lengths for these data.

## IMPACT/APPLICATIONS

The procedures presented here allow SAR wave imagery to be used to gather statistics on wave coherence. These in turn can provide realistic wave coherence statistics to aid in the design of large offshore structures.

**RELATED PROJECTS.** “Synthetic Aperture Radar Imagery of the Ocean Surface During the Coastal Mixing and Optics Experiment,” Donald Thompson and David Porter

## REFERENCES

- [1] C. Elachi and W. Brown Jr. Models of radar imaging of ocean surface waves. *IEEE Trans. Antennas Propag.*, AP-25:84–95, 1977.
- [2] W. Alpers, D. Ross, and C. Rufenach. On the detectability of ocean surface waves by real and synthetic aperture radar. *J. Geophys. Res.*, 95:6481–6498, 1981.
- [3] R. Beal, F. Monaldo, D. Tilley, D. Irvine, E Walsh, F. Jackson, D. Hancock III, D. Hines, R. Swift, F. Gonzalez, D. Lyzenga, and L. Zambresky. A comparison of SIR-B directional wave spectra with aircraft scanning radar spectra. *Science*, 232:1531–1535, 1986.
- [4] K. Hasselmann, R. Raney, W. Plant, W. Alpers, W. Shuchman, D. Lyzenga, C. Rufenach, and M. Tucker. Theory of synthetic aperture radar ocean imaging: A MARSEN view. *J. Geophys. Res.*, 90:4659–4686, 1985.
- [5] F. Monaldo and D. Lyzenga. On the estimation of wave slope- and height-variance spectra from SAR imagery. *IEEE Geosci. Remote Sensing*, GE-24: 543–551, 1986.
- [6] C. Swift and L. Wilson. Synthetic aperture radar imaging of ocean waves. *IEEE Trans. Antennas Propag.*, AP-27:725–729, 1979.
- [7] W. Alpers and C. Rufenach. The effect of orbital velocity motions on the synthetic aperture imagery of ocean waves. *J. Geophys. Res.*, AP-27:685–690, 1979.
- [8] F. Monaldo. Estimating wave groupiness using the autocorrelation function. *JHU/APL Tech. Rep. SRO–99–03*, The Johns Hopkins University Applied Physics Laboratory, Laurel, MD, 1999.

## PUBLICATIONS

- F. Monaldo. Measuring the properties of wave coherence with SAR, *Mobile Offshore Base Technology Exchange Conference*. Arlington, VA, March 16–18, 1999.
- F. Monaldo. Measurement of ocean spatial coherence by spaceborne Synthetic Aperture Radar. *1999 Very Large Floating Structures Conference*. Honolulu, Hawaii, September 22–24, 1999.
- F. Monaldo. Status Report for the MOB Technology Assessment Report SAR Measurements of Wave Coherence. *JHU/APL Report SRO–99–08*, July 1999.
- F. Monaldo. Estimating Wave Groupiness Using the Autocorrelation Function. *JHU/APL Report SRO–99–03*, January 1999.
- F. Monaldo. Blobs Best Wave Crests or Ellipses Estimate Crest Elongation. *JHU/APL Tech. Memo. SRO–98M–33*, December 1998.